Biosensors and Bioelectronics 80 (2016) 194–200

Contents lists available at ScienceDirect

Biosensors and Bioelectronics

journal homepage: www.elsevier.com/locate/bios

Label-free impedimetric biosensor for *Salmonella Typhimurium* detection based on poly [pyrrole-co-3-carboxyl-pyrrole] copolymer supported aptamer

E. Sheikhzadeh [a,b], M. Chamsaz [b], A.P.F. Turner [a], E.W.H. Jager [a], V. Beni [a,*]

[a] Biosensors & Bioelectronics Centre, Dept. of Physics, Chemistry and Biology (IFM), Linköping University, Linköping, Sweden
[b] Department of Chemistry, Faculty of Science, Ferdowsi University of Mashhad, Mashhad, Iran

ARTICLE INFO

Article history:
Received 6 December 2015
Received in revised form
19 January 2016
Accepted 21 January 2016
Available online 22 January 2016

Keywords:
S. Typhimurium
Aptamer
Electrochemical impedance spectroscopy
Poly [pyrrole-co-3-carboxyl-pyrrole]
Label-free detection

ABSTRACT

The Gram-negative bacterium, *Salmonella Typhimurium (S. Typhimurium)* is a food borne pathogen responsible for numerous hospitalisations and deaths all over the world. Conventional detection methods for pathogens are time consuming and labour-intensive. Hence, there is considerable interest in faster and simpler detection methods.

Polypyrrole-based polymers, due to their intrinsic chemical and electrical properties, have been demonstrated to be valuable candidates for the fabrication of chemo/biosensors and functional surfaces. Similarly aptamers have been shown to be good alternatives to antibodies in the development of affinity biosensors.

In this study, we report on the combination of poly [pyrrole-co-3-carboxyl-pyrrole] copolymer and aptamer for the development of a label-less electrochemical biosensor suitable for the detection of *S. Typhimurium*. Impedimetric measurements were facilitated by the effect of the aptamer/target interaction on the intrinsic conjugation of the poly [pyrrole-co-3-carboxyl-pyrrole] copolymer and subsequently on its electrical properties. The aptasensor detected *S. Typhimurium* in the concentration range 10^2–10^8 CFU mL^{-1} with high selectivity over other model pathogens and with a limit of quantification (LOQ) of 100 CFU mL^{-1} and a limit of detection (LOD) of 3 CFU mL^{-1}. The suitability of the aptasensor for real sample detection was demonstrated via recovery studies performed in spiked apple juice samples. We envisage this to be a viable approach for the inexpensive and rapid detection of pathogens in food, and possibly in other environmental samples.

1. Introduction

The Gram-negative bacterium *Salmonella* is a major food borne pathogen for humans and animals. This pathogen is known as a major factor in gastrointestinal infections and is associated with numerous hospitalisations and deaths all over the world. *Salmonella* can be found in meat, eggs, milk and beverage. Among the over 2500 serotypes of *Salmonella*, one of the most common serotype related to human disease is *Salmonella enterica serovar typhimurium* (*S. Typhimurium*) (Kim et al., 2015; Lee et al., 2015; Ma et al., 2014). Traditional methods of detection of this pathogen are based on the combination of pre-enrichment steps, culturing on *Salmonella-Shigella* (SS) agar plates, and serological validation of suspicious colonies. Although these approaches can provide reliable results, they are quite time consuming and can take up to 5 days to obtain a result. Due to these drawbacks, the development of new and faster approaches for bacteria detection is a core activity in contemporary microbiology (Lee et al., 2015).

Immunological assays such as ELISA can detect *Salmonella* at level of 10^4–10^5 cells mL^{-1}; and lower detection levels can be achieved by coupling ELISA methods with an enrichment step that usually takes between 16 and 24 h (Alakomi and Saarela, 2009; Xu et al., 2015). Polymerase chain reaction (PCR)-based methods have been shown to significantly improve the limit of detection down to 5 CFU (colony forming unit) mL^{-1}, but still these approaches require long and often complicated preparation steps, such as cell lysis and, often, DNA separation. Furthermore these methods do not have the ability to determine the viability of the pathogen at the time of the sampling (Zelada-Guilln et al., 2009; Zourob et al., 2008). Despite significant advances, current *Salmonella* detection methods are not fast, easy to perform, reliable or sensitive enough (Lee et al., 2015).

Conductive conjugated polymers (CP) are very attractive and

* Corresponding author. Current address: ACREO SWEDISH ICT AB, Box 787, SE-601 17 Norrköping, Sweden.
E-mail address: valerio.beni@acreo.se (V. Beni).

http://dx.doi.org/10.1016/j.bios.2016.01.057
0956-5663/

versatile materials for the fabrication of functional interfaces and sensing surfaces. They combine the properties of metals and those of conventional polymer and have found application in various areas including extraction methods (Bagheri et al., 2013), fuel cells (Inamuddin et al., 2009), artificial muscles (Jager et al., 2000) and biomedical engineering (Guimard et al., 2007) as well as in chemosensors (Pattananuwat et al., 2015), biosensors (Li et al., 2015) and functional surfaces for cell stimulation(Svennersten et al., 2011), tissue engineering (Svennersten et al., 2011) and bacterial differentiation (Golabi et al., 2016a).

Among CPs, polypyrrole has found widespread application due to properties such as ease of synthesis in different solvents and at room temperature, good chemical stability and high conductivity. Even more interestingly, polypyrrole can be fabricated via electrochemical approaches, giving a high degree of control over thickness, shape, morphology and hydrophobicity (Balint et al., 2014; Janmanee et al., 2013; Kannan et al., 2011; Peng et al., 2007). However, polypyrrole suffers from the absence of functional groups and so copolymerisation of pyrrole with modified monomers has been explored as a possible route to provide polypyrrole films with new functionalities (Melling et al., 2015).

Copolymers such as poly[pyrrole-co-4-(3-pyrrolyl)] butanoic acid, have been used for the fabrication of DNA hybridisation biosensors (Peng et al., 2005). DNA chips, fabricated using poly [pyrrole-COOH-co-pyrrole-DNA probe] copolymer, were used to detect DNA at levels as low as 10^{-15} mol mL^{-1} (Garnier et al., 2007; Wallace et al., 1997) and the copolymer, poly[pyrrole-co-3-pyrrolylacrylic acid], has been used for the development of impedimetric genosensors (Peng et al., 2007).

Aptamers are short sequences of DNA or RNA that have the ability to bind with high affinity and specificity to their target. They are considered to have several advantages over their corresponding antibodies including small size, ease of synthesis and labelling, low cost of production and the absence of the need for animals to produce them (Zhu et al., 2012).

Electrochemical detection methods are widely used because of their ease of operation, high sensitivity and ready miniaturisation for use in portable device (Zhu et al., 2012). For example, an electrochemical immunosensor based on screen-printed gold electrodes, was developed for the chronoamperometric detection of *S. Typhimurium* down to 20 cell mL^{-1}(Salam and Tothill, 2009). Zelada-Guillén et al. (2012) demonstrated the real-time potentiometric detection of *Staphylococcus aureus* in pig skin by the use of carbon nanotube/aptamer functionalised electrodes. Anodic stripping voltammetry was used for electrochemical dual-aptamer-based, sandwich detection of *Staphylococcus aureus* down to 1 CFU mL^{-1} (Abbaspour et al., 2015). Finally, a target-induced aptamer displacement strategy has been applied for the detection of *E. coli O111* via differential pulse voltammetry (Luo et al., 2012).

Label-free electrochemical detection is a very attractive option and has been demonstrated by the use of electrochemical impedance spectroscopy. For example an electrochemical impedance aptasensor for *S. Typhimurium* was constructed based on graphene oxide/gold nanoparticles and was able to detect the pathogen in the concentration range 2.4–2.4 × 10^3 CFU mL^{-1} (Ma et al., 2014). Furthermore, a screen-printed interdigitated microelectrode, in combination with magnetic-bead sample separation was applied for the rapid detection of *E. coli O157:H7* and *S. Typhimurium* in food samples (Xu et al., 2015). In addition, Labib et al., developed an aptamer-based impedimetric sensor with the ability to detect *S. enteritidis* down to 600 CFU mL^{-1} in 10 min, and to distinguish it from other Salmonella species, including *S. typhimurium* and *S. choleraesuis* (Labib et al., 2012a). The same authors developed an impedimetric sensor via the self-assembly of thiolated aptamer onto a gold nanoparticle-modified screen-printed electrode. The tunable specificity of the aptamers, allowed live and killed bacteria be distinguished (Labib et al., 2012b).

Unfortunately however, all the label-free electrochemical approaches described above required the presence of a redox probe, more often ferro/ferricyanide, in the measuring solution. In the study presented herein, we report on the use of the poly[pyrrole-co-3-carboxyl-pyrrole] copolymer-aptamer bioconjugated for the development of a label-free electrochemical biosensor for the detection of *S. Typhimurium* based on the intrinsic variation of the electrical properties of the polymeric surface, without the need for the addition of redox probes. The potentiality of the proposed aptasensor was demonstrated via calibration, selectivity and recovery experiments, which demonstarted its specificity, sensitivity and applicability for the detection of *S. Typhimurium* in a food sample (apple juice).

2. Experimental

2.1. Materials

Analytical grade reagents without further purification, except for pyrrole monomer (vacuum distilled prior to use), were used in this work.

Pyrrole-3-carboxylic acid (Py-COOH) was purchased from Fluoro chem (Hadfield United Kingdom) and lithium perchlorate ($LiClO_4$) from Acros. N-hydroxysuccinimide (NHS), N-(3-dimethylaminopropyl)-N′-ethylcarbodiimide hydrochloride (EDC) and Pyrrole (Py) were obtained from Sigma-Aldrich (Stockholm, Sweden). PBS (pH 7.4) tablets were supplied by Medicago AB (Uppsala, Sweden).

The six bacterial strains used in this study were: Escherichia Coli (CCUG 3274, CCUG53375, and CCUG10979), Entrobacter aerogenes and Citrobacter freundii) and *S. Typhimurium.* The three *E. Coli* strains were acquired from the Culture Collection, University of Gothenburg, Sweden, the other strains were provided, in kind, by Linköping University Hospital.

Aptamer with 5′-NH_2-ttt ggt cct tgt ctt atg tcc aga atg cga gga aag tct ata gca gag gag atg tgt gaa ccg agt aaa ttt ctc cta ctg gga tag gtg gat tat-3′ sequence (N 45 in the original manuscript) was obtained from a previous work reported by Joshi et al. (2009). The synthetic aptamer was purchased lyophilised from biomers.net (Germany). On arrival, the aptamer was reconstituted to a 100 μM stock solution with filtered (0.2 μm filter) Milli-Q water, divided in small aliquots and stored at −20 °C until use.

All solutions were prepared in high purity water obtained from a Milli-Q RG system (Stockholm, Sweden).

2.2. Apparatus

An Ivium Stat.XR electrochemical analyser coupled with dedicated software (Ivium, Eindhoven, Netherlands) was used for electrochemical measurements, film deposition and cleaning of the gold surface. Attenuated total reflectance (ATR-FTIR) measurements were done with a PIKE MIRacle ATR accessory with a diamond prism in a Vertex 70 spectrometer (Bruker) using a DTGS detector; all measurements were performed at room temperature under continuous purging of N_2. IR spectra were obtained at 4 cm^{-1} resolution and 32 scans between 4000 and 800 cm^{-1}. The Scanning Electron Microscopy (SEM) micrographs were taken using a Leo 1550 Gemini SEM operating at 6.0 keV.

A Shimadzu UV-1601 PC spectrophotometer was used to obtain the concentration of cultured bacteria (600 nm). Contact angle measurements were carried out using a CAM 200 optical contact angle metre (KSV Instrument, Helsinki, Finland).

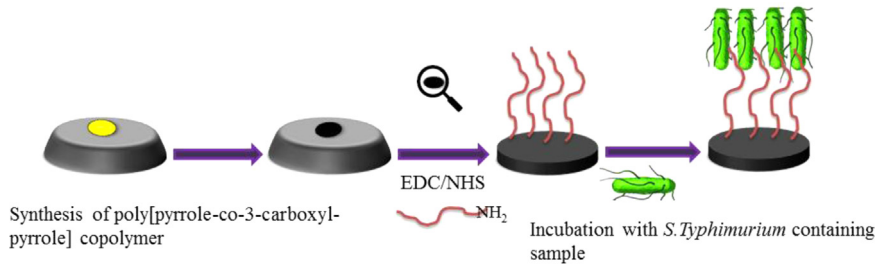

Scheme1. Pictorial representation of the proposed approach for aptsensor fabrication.

2.3. Preparation of the film

Gold disk electrodes (internal diameter 2 mm from CHI Instruments), USA) were polished on polishing pad micro clothes with 1.0, 0.3 and 0.05 μm alumina powder (CHI Instruments, USA) to a mirror finish and then cleaned in a water ultrasonic bath. After the mechanical cleaning, the surface was immersed for 60 s in cold piranha solution (3:1 H_2SO_4/H_2O_2) followed by an electrochemical activation step in H_2SO_4 (0.5 M) solution by cyclic voltammetry (25 cycles).

A copolymer of Pyrrole-3-carboxylic acid and Pyrrole (1:4 ratio in 100 mM $LiClO_4$ aqueous solution) was synthesised using a potentiostatic (constant potential) method at 0.7 V (vs Ag/AgCl, KCl 3 M reference electrode) until the consumed charge reached 5 mC cm^{-2}. The prepared film was washed with deionised water and stored at 4 °C until use.

For SEM and FT-IR images, the same procedure was applied on 5×10 mm^2 Au chips produced by sputtering a 2000 Å Au film onto a Ti coated (100 Å) Si wafer.

2.4. Immobilisation of aptamer onto polymeric film

The presence of the carboxylic group in the poly[pyrrole-co-3-carboxyl-pyrrole] copolymer films allowed the covalent immobilisation of the aptamer (Chei et al., 2008; Tlili et al., 2005). Functionalisation of the copolymer with aptamers was carried out by immersing the film in 40 μL aqueous solution containing 50 mM NHS and 200 mM EDC for 30 min, in order to activate the carboxylic group present,; this was, followed by incubation of the activated film with 20 μL of a 2 μM aqueous solution of the amino-functionalised aptamer for 60 min.

2.5. Preparation of bacterial solution

The six bacterial strains were cultured separately in Tryptic Soy Broth (TSB) for 18 h, at 37 °C under gentle (170 rpm) shaking. The overnight cultured bacterial cells were then collected by centrifugation (5 min at 5000*g*), the supernatant discarded and the pellet resuspended in sterile phosphate buffered saline (PBS) solution (pH 7.4). Following three cycles of washing (accordingly to the procedure described above) the bacterial solutions were diluted to 10^8 CFU mL^{-1} (concentration calculated according to Mc Farland turbidity standards); these solutions were used as the working stock bacterial solutions. Serial dilutions (10^2–10^8 CFU/mL) of standard stock solutions were prepared with $LiClO_4$ 100 mM for measurement.

2.6. Impedance measurement

The impedance measurements were recorded from 10 kHz to 0.5 Hz, at amplitude of 5 mV, in 100 mM $LiClO_4$ solution without any redox probe. All measurements were performed at a bias potential of 0 mV vs the OCP (open circuit potential) of the film.

Measurement in the presence of the redox probing molecule (5 mM Ferro/Ferri equimolar solution) were also attempted; this resulted to be less reproducible and noisier (data not shown) making in this way favourable the measurements in 100 mM $LiClO_4$ solution alone.

2.7. Bacteria measurements

Detection of bacteria was performed accordingly to the following protocol: aptasensor were incubated for 45 min in the $LiClO_4$ 100 mM solution containing the bacteria or in the 1–100 diluted apple juice. Following a 15 min wash in $LiClO_4$ 100 mM the EIS spectra were recorded accordingly to protocol described in Section 2.6. Calibration curve were performed by exposing the aptasensor to increasing concentrations from 10^2 to 10^8 CFU mL^{-1} of *S. Typhimurium*. For each concentration measurements were performed following the protocol described above. Following recording the EIS spectra the aptasensors were put in contact with the solution containing the following higher concentration to be investigated (Scheme 1).

3. Results and discussion

3.1. Characterisation of copolymer

3.1.1. Scanning electron microscopy (SEM)

Fig. 1 shows the SEM images (low and high resolution) of a polypyrrole (PPy) (Fig. 1A and B) and poly[pyrrole-co-3-carboxyl-pyrrole] copolymer (Fig. 1C and D) films synthesised according to the protocol described in the Section 2. Clearly the two surfaces showed different morphology; poly[pyrrole-co-3-carboxyl-pyrrole] copolymer film presented a smoother structure when compared with the PPy (Guimard et al., 2007). The PPy film was characterised by the well-known globular and compact structure of PPy The smoother surfaces recorded in the case of the poly [pyrrole-co-3-carboxyl-pyrrole] copolymer film could be due to the reduced polymerisation speed (ca. 2.5 times slower than those of PPy) (Xu et al., 2005; Street et al., 1983; Golabi et al., 2016b) and to the presence of the COOH that introduced into the copolymer chain sterical and electrostatic hindrances (Korri-Youssoufi and Yassar, 2001) resulting in a more planar, more flat linear chain.

3.1.2. ATR-FTIR spectroscopic measurements

Copolymer formation was further confirmed by ATR-FTIR spectroscopic measurements (Fig. 1E). The poly[pyrrole-co-3-carboxyl-pyrrole] copolymer (blue line) showed a peak at 1680 cm^{-1}, which is associated with the C=O stretching mode of carboxylic groups (Peng et al., 2005) and which is clearly absent in the PPy film (red line). Furthermore a shift to higher frequencies of FT-IR spectrum of poly[pyrrole-co-3-carboxyl-pyrrole]copolymer was recorded; this was an indication of the reduced rotational freedom in the polymer probably due to the changes in the polymer backbone associated with the presence of COOH in it.

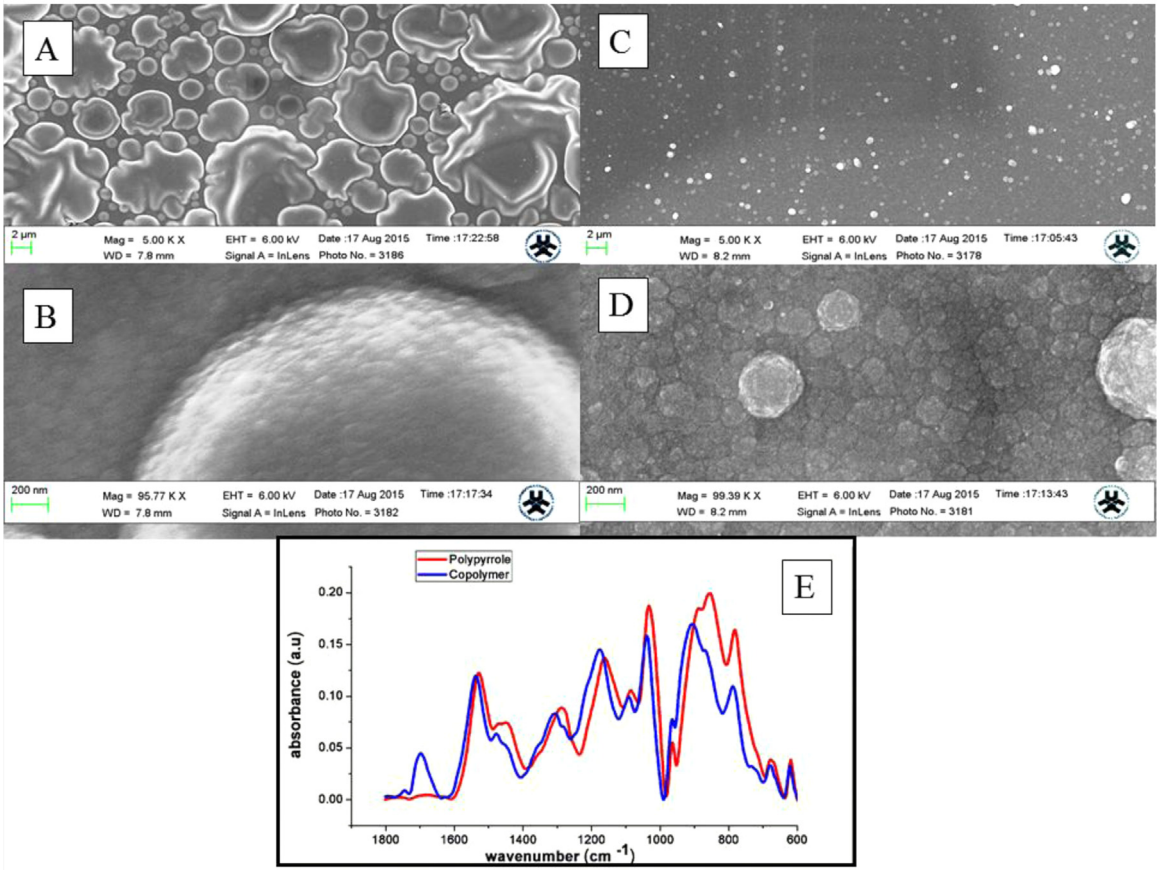

Fig. 1. SEM image (low and high resolution) of PPy (A and B) and poly[pyrrole-co-3-carboxyl -pyrrole] copolymer (C and D) deposited onto Silicon based Au film. FT-IR spectrum of (E) poly[pyrrole-co-3-carboxyl-pyrrole] copolymer (blue line) and PPy (red line) films. (For interpretation of the references to colour in this figure legend, the reader is referred to the web version of this article.)

3.1.3. Cyclic voltammetry measurements

Electrochemical characterisation of the prepared films was performed using cyclic voltammetric and impedimetric measurements. Cyclic voltammograms of the prepared films were recorded in $LiClO_4$ 100 mM solution; these experiments allowed a deeper understanding of the redox properties of the films (Fig. 2A). The poly[pyrrole-co-3-carboxyl-pyrrole] copolymer showed two distinct couples of redox peaks ($-0.5/-0.6$ V and $-0.15/-0.16$ V) attributed, respectively, to the pyrrole–COOH unit and to the pyrrole monomer oxidation/reduction (Chei et al., 2008). On the other hand, when cyclic voltammetric experiments were recorded for the PPy film, only a pair of redox peaks at -0.15 V and -0.16 V was recorded. Another significant difference was that the poly [pyrrole-co-3-carboxyl-pyrrole] copolymer showed a quasi-reversible behaviour, while the PPy demonstrated reversible behaviour; these changes in redox properties could be associated with the reduced conductivity of the film, loss in polymer chain conjugation (Garnier et al., 2007; Wallace et al., 1997), when the monomer with the COOH group was incorporated in the film (Chei et al., 2008). This difference recorded in the voltammetric spectra

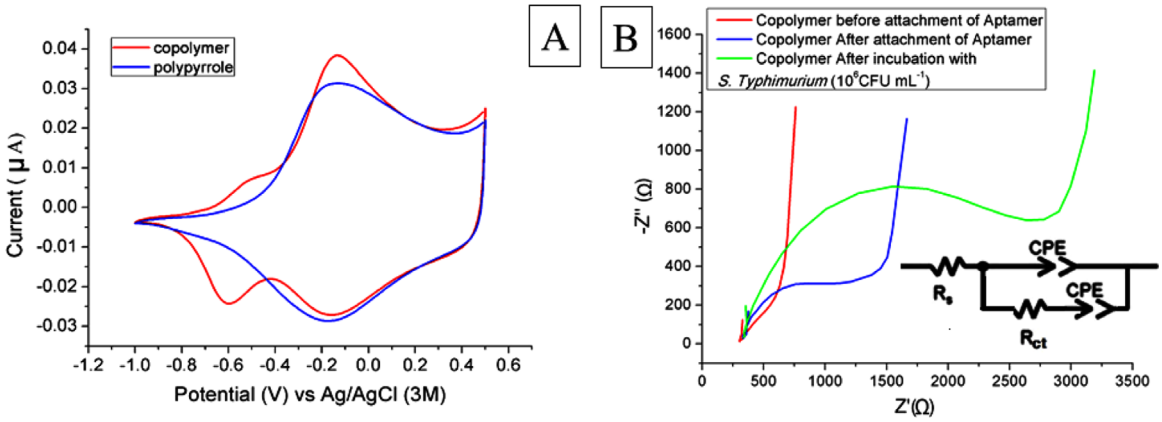

Fig. 2. (A) Cyclic voltammogram of poly[pyrrole-co-3-carboxyl-pyrrole] copolymer (red line) and PPy (blue line) in $LiClO_4$ 100 mM at 50 mVs^{-1}. (B) EIS measurements of poly [pyrrole -co- 3-carboxyl -pyrrole] copolymer film before (red line) and after (blue line) attachment of aptamer and after incubation with 10^6 CFU mL^{-1} solution of *S. Typhimurium* (green line) (measurement solution $LiClO_4$ 100 mM). The impedance spectra were recorded from 10 kHz to 0.5 Hz, at 0 mV vs (OCP), amplitude of 5 mV in $LiClO_4$ 100 mM solution. (For interpretation of the references to colour in this figure legend, the reader is referred to the web version of this article.)

confirms the successful electrodeposition of the poly[pyrrole-co-3-carboxyl-pyrrole] copolymer and that this has a block-polymer form (Korri-Youssoufi and Yassar, 2001).

3.1.4. Contact angle measurement

Contact angle measurements were used to study the wettability properties of the surface. The poly[pyrrole-co-3-carboxyl-pyrrole] copolymer showed a reduced contact angle when compared to the PPy film (Table 1S). This reduction in contact angle is a clear indication of the increased hydrophilic character of the copolymer. This increased hydrophilicity was ascribed to the presence of the carboxylic acid groups and to their ability to form hydrogen bonds with the water (Truong et al., 2011).

3.1.5. Impedance measurement

Impedance measurements showed a reduced intrinsic conductivity (increase in resistance) of the poly[pyrrole-co-3-carboxyl-pyrrole] copolymer when compared to the PPy film (Fig. 1S). The presence of the COOH groups in the copolymer chain is expected to introduce a sterical and electrostatic hindrance that is expected to affect the conjugation in the polymeric film. Alteration of the π–π conjugation in PPy films has been shown to have a significant effect on the film conductivity (Garnier et al., 2007; Wallace et al., 1997).

3.2. Aptamer immobilisation

The Au electrodes modified with poly[pyrrole-co-3-carboxyl-pyrrole] copolymer film were used to develop aptasensors via covalent immobilisation of the aptamer onto the surface using EDC/NHS chemistry (methods section). In this step high concentration of amino modified aptamer (2 μM) was used with the aim of saturating with aptamer the copolymer. Immobilisation of aptamer onto the surface was confirmed by contact angle measurement (Table 1S) and electrochemical impedance measurements (Fig. 2B). The presence of phosphate groups in the aptamer structure was considered, responsible for the increased hydrophilicity of the poly[pyrrole-co-3-carboxyl-pyrrole] copolymer-aptamer surface, which was clearly highlighted by the reduced contact angle value (Table 1S). This result was confirmed by EIS measurement (Fig. 2B). A general circuit was utilised to model the impedance spectrum (inset Fig. 2B). In the proposed circuit, previously described by Tlili et al. (2005), Rs represents the solution resistance, Rct is the charge transfer resistance at the copolymer-aptamer/electrolyte interface, and CPE is the constant phase element accounting for the charge capacitance at the copolymer-aptamer/electrolyte interface. The model was shown to fit adequately the response obtained for the different surfaces investigated including poly[pyrrole-co-3-carboxyl-pyrrole] copolymer and poly[pyrrole-co-3-carboxyl-pyrrole] copolymer-aptamer bioconjugate and for the sensor response upon detection of *S. Typhimurium* at the different concentration investigated. This could be clearly seen from Fig. 2S where example of the fitting results are presented.

The value of Rct changed significantly following aptamer immobilisation, passing from ca. 78 Ω for the poly[pyrrole-co-3-carboxyl-pyrrole] copolymer, to ca. 1118 Ω for the poly poly[pyrrole-co-3-carboxyl-pyrrole] copolymer-aptamer bioconjugated film. This result was consistent with previous report where the aptamer attachment was associated with an increase in the resistance of the polymer (Zhu et al., 2012).

3.3. Detection of bacteria

Different concentration of bacteria solutions (10^2–10^8 CFU mL^{-1}) were prepared by dilution of bacterial stock solutions in $LiClO_4$ 100 mM. The choice of $LiClO_4$ was dictated by the fact that incubation (45 min) in PBS (the buffer in which the aptamer was selected) (Joshi et al., 2009) resulted in a significant alteration of the conductivity properties of the poly[pyrrole-co-3-carboxyl-pyrrole] copolymer-aptamer film, as clearly indicated by the EIS measurements reported in the Supporting Information (Fig. 3S).

The suitability of $LiClO_4$ solution for bacteria detection was investigated by comparing the EIS results before and after the incubation of poly[pyrrole-co-3-carboxyl-pyrrole] copolymer-aptamer-films with 100 mM $LiClO_4$ solution with (10^6 CFU mL^{-1}) and without *S. Typhimurium*. As can be seen from Fig 4S, when bacteria were absent, there was no significant change in the impedimetric response. On the other hand, when bacteria were present, a clear increase in the impedance response was recorded (Fig. 2B). Interaction between the aptamer and bacteria is expected to induce significant changes in the poly[pyrrole-co-3-carboxyl-pyrrole] copolymer-aptamer-films electrical properties by altering significantly the environment in close proximity with polymeric chains (Peng et al., 2009; Tlili et al. 2005). Several phenomena have been shown to alter the intrinsic conductivity properties of CPs including: (i) alteration of the π–π conjugation (Garnier et al., 2007; Wallace et al., 1997) due to the steric hindrance generated by the introduction, following biorecognition, in the polymer body of the bulky bioorganism, (ii) changes in the interfacial double layer due to the charge properties of the pathogens (Zelada-Guilln et al., 2009) and (iii) reduction in the mobility of the dopant (ClO_4^-) due to the electrostatic repulsion induced by the pathogens (Thompson et al., 2003).

In order to confirm the role of the aptamer in the performance of the biosensor, two control experiments were performed. In the first experiment, poly[pyrrole-co-3-carboxyl-pyrrole] copolymer film without immobilised aptamer were incubated with (10^4 CFU mL^{-1}) bacterial solution. In the second experiment, a biosensor modified with an *E.Coli*-specific aptamer (Bruno, 2014), was incubated with the same concentration of bacteria. The results of these control experiments (Figs. 5S and 6S, respectively) clearly showed limited response, probably due to physical absorption of bacteria onto the polymeric surface, when compared to those recorded with the proposed *S. Typhimurium* aptasensor.

3.4. Optimisation of incubation time for S. Typhimurium detection

Prior to evaluating the analytical performance, in terms of response/concentration and selectivity, the influence of the incubation time on the aptasensor response was evaluated. In order to explore this, aptasensors were incubated with bacterial solution (10^6 CFU mL^{-1}) for different incubation times (Fig 7S). In order to minimise the variability that can be recorded between different aptasensor the relative variation of Rct (ΔRct/Rct0) was used as analytical response (Nasef et al., 2010). This value was calculated as follows:

$$\Delta Rct/Rct0 = (Rct_{after} - Rct0)/Rct0 \quad (1)$$

where Rct_{after} is the value of Rct after recognition of the pathogen and Rct0 is the value recorded for the poly[pyrrole-co-3-carboxyl-pyrrole] copolymer-aptamer-films before the incubation with the solution containing the pathogen.

As it can be seen from Fig 8S, the analytical response increased until 45 min when it started to level off. A longer incubation time (60 min) did not result in a significant increase in the response; subsequently 45 min was selected as incubation time for the following experiments.

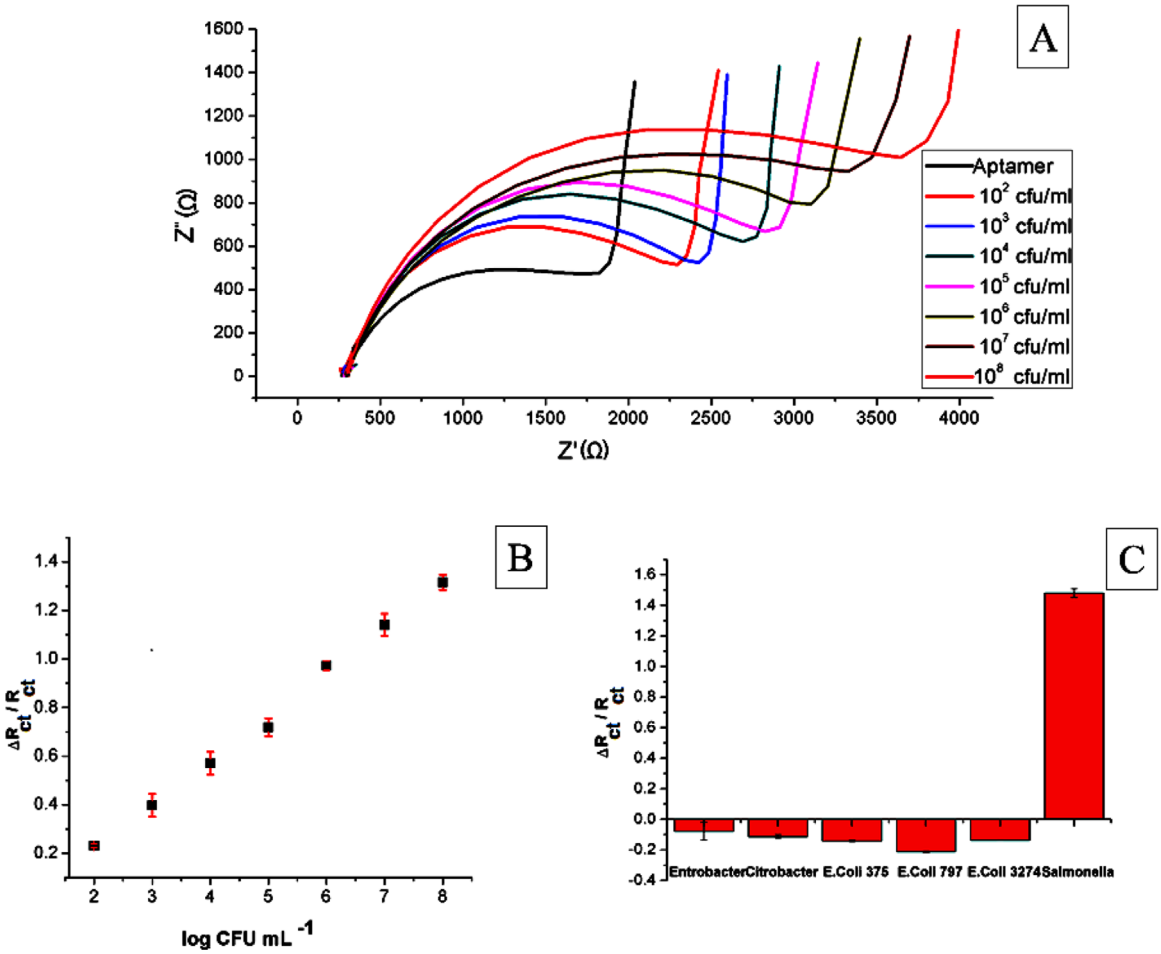

Fig. 3. (A) Impedance measurement for different concentrations (10^2–10^8 CFU mL^{-1}) of *S. Typhimurium;* (B) Calibration curve obtained by fitting the results from 3 consecutive calibration curves. (C) Selectivity evaluation of the aptasensor over the detection of six model pathogens 3 *E. Coli* strains, *Enterobacter* and *Citrobacter* (10^6 CFU mL^{-1}) Measurement and capture solution: $LiClO_4$ 100 mM. Error bars (Fig. 3B and C) were obtained by calculating the SD of 3 measurements performed each with a different aptasensors. The impedance spectra were recorded from 10 kHz to 0.5 Hz, at 0 mV vs (OCP), amplitude of 5 mV in $LiClO_4$ 100 mM solution.

3.5. *S. Typhimurium calibration curve*

Calibration curves were built following the protocol described in the material and method section (Section 2.1). Typical aptasensor responses are illustrated in Fig. 3A and a calibration plot is presented in Fig. 3B. The relative resistance was shown to increase linearly ($y=0.1566x-0.0382$ equation with $R^2=0.99$) with the logarithm of the *S. Typhimurium* concentration within the investigated concentration interval (range of 10^2– 10^8 CFU mL^{-1}) with a LOQ of 10^2 CFU mL^{-1} and a LOD (3 time the standard detection of the blank experiment: incubation in the absence of *S. Typhimurium*) of 3 CFU mL^{-1}. Error bars in the calibration indicate the reproducibility (3 measurements), over 2 days, performed using 3 different aptasensors.

Reproducibility of the aptasensor was calculated over the full range of concentration; this resulted in an average RSD of 5.2% ($n=3$ for each of the 7 concentrations used in this calculation and listed in Table 2S).

3.6. *Selectivity of the aptasensor*

Three different strains of *E. Coli*, *Enterobacter* and *Citrobacter* were utilised to investigate the specificity of the aptasensor. Solutions containing 10^6 CFU mL^{-1} of each bacterium were incubated with the aptasensor for 45 min. As it can be seen from Fig. 3C, the relative resistances (calculated accordingly to Eq. (1)) for the five investigated bacteria strains are much lower than those recorded for the *S. Typhimurium*, confirming the specificity of the aptasensor. Interestingly is the fact that for interfering strain resulted in a loss of Rct; the reason for these results are not clear but they might reside in the intrinsic charge and morphological properties of the different pathogens.

3.7. *Real sample measurement*

Real sample measurements were carried out in spiked (10^2 and 10^6 CFU mL^{-1}) filtered and diluted apple juice. Dilution of the apple juice (1–100) was performed using $LiClO_4$ 100 mM as dilution media. The results of the recovery studies are summarised in Table 1. Concentrations of bacteria in the spiked samples were calculated by fitting the relative resistance (calculated accordingly to Eq. (1)) variation in the calibration curve of Fig. 3B. Clearly the aptasensor worked in diluted spiked real samples. Reproducibility of the detection was calculated for both spiked concentration ($n=3$); this resulted in an average RSD of 11%.

Table 1
Summary of recovery studies in 1:100 diluted, in $LiClO_4$ 100 mM, apple juice.

Nominal concentration CFU mL^{-1}	Experimentally obtained concentration CFU mL^{-1}
10^2	1.4×10^2
10^6	4.1×10^6

4. Conclusions

In this study the successful fabrication of the poly [pyrrole-co-3-carboxyl-pyrrole] copolymer and its conjugation with a *S. Typhimurium* specific aptamer was achieved. Chemical (FT-IR) physical (electrochemical and contact angle) characterisations were used to confirm the synthesis of the designed bioconjugate film. The use of the poly [pyrrole-co-3-carboxyl-pyrrole] copolymer-aptamer bioconjugate as sensing surface in electrochemical impedance label-free aptasensor was also investigated. The proposed method sensing surface was demonstrated to allow sensitive detection of *S. Typhimurium* in a fast and sensitive way by taking advantage of the changes, following aptamer pathogen interaction, in the electrical properties of the poly [pyrrole-co-3-carboxyl-pyrrole] copolymer without the need of the addition of any reporting redox probe. This significantly simplifies the assay opening in this way new possibility for fast in situ screening of environmental and food products. The developed label-free aptasensors was shown to respond linearly over the *S. Typhimurium* concentration range 10^2–10^8 CFU mL^{-1} with a LOQ of 10^2 CFU mL^{-1} and a LOD of 3 CFU mL^{-1}. The aptasensor was also shown to be highly selective for *S. Typhimurium* when compared to the detection of other possible model interfering strains (*E. coli* 375, *E.coli 797*, *E.coli 3274*, *Enterobacter*, *Citrobacter).* Finally the aptasensor was demonstrated to allow the fast (45 min) label-free detection of *S. Typhimurium* in spiked apple juice. Despite further work on the stabilisation of the sensor surface will be required, the authors envisage this as a viable approach for inexpensive, simple and rapid detection of pathogens in food and possibly environmental samples.

Acknowledgements

The authors are thankful to Mr. Mohsen Golabi for his kind help with the bacterial culturing and experiments and contact angle measurement. ES would like to acknowledge the Ministry of Science Research and Technology of Iran and Research Council of Ferdowsi University of Mashhad (Research project no. 3/29828) to support her research exchange to Linköping University. AT, VB and EJ would like to thank Linköping University, Vetenskapsrådet (Pathoscreen project; Swedish Research Link; ref.-ID: D0675001) and the Swedish Research Council (contract nr VR-2014-3079) for financial support.

Appendix A. Supplementary material

Supplementary data associated with this article can be found in the online version at http://dx.doi.org/10.1016/j.bios.2016.01.057.

References

Abbaspour, A., Norouz-Sarvestani, F., Noori, A., Soltani, N., 2015. Biosens. Bioelectron. 68, 149–155.
Alakomi, H.L., Saarela, M., 2009. Qual. Assur. Saf. Crop. Foods 1, 142–152.
Bagheri, H., Ayazi, Z., Naderi, M., 2013. Anal. Chim. Acta 767, 1–13.
Balint, R., Cassidy, N., Cartmell, J., H, S., 2014. Acta Biomater. 10, 2341–2353.
Garnier, F., Bouabdallaoui, B., Srivastava, P., Mandrand, B., Chaix, C., 2007. Sens. Actuators B 123, 13–20.
Bruno, J.G., 2014. Pathogens 3 (2), 341–355.
Chei, W., Lu, Z., Li, C.M., 2008. Anal. Chem. 80, 8485–8492.
Golabi, M., Turner, A.P.F., Jager, E.W.H., 2016a. Sens. Actuators B: Chem. 222, 839–848.
Golabi, M., Turner, A.P.F., Jager, E.W.H., 2016b. Macromol. Chem. Phys, http://dx.doi.org/10.1002/macp.201500445 (In press).
Guimard, N., Gomez, K., Schmidt, N., E, C., 2007. Prog. Polym. Sci. 32, 876–921.
Inamuddin, Shin K.M., Kim, S.,I., Insuk, So, Kim, S.J., 2009. Electrochim. Acta 54, 3979–3983.
Jager, E.W.H., Smela, E., Inganäs, O., 2000. Science 290 (5496), 1540–1545.
Janmanee, R., Baba, A., Phanichphant, S., Sriwichai, S., Shinbo, K., Kato, K., Kaneko, F., 2013. Mol. Cryst. Liq. Cryst. 580 (1), 29–34.
Joshi, A., Janagama, H., Dwivedi, H.P., Senthil Kumar, T.M.A., Jaykus, L.-A., Schefers, J., Sreevatsan, S., 2009. Mol. Cell. Probes 23, 20–28.
Kannan, B., Williams, David E., Marsilea, A. Booth, Travas-Sejdic, J., 2011. Anal. Chem. 83, 3415–3421.
Kim, G., Moon, J., Moh, C., Lim, J., 2015. Biosens. Bioelectron. 67, 243–247.
Korri-Youssoufi, H., Yassar, A., 2001. Biomacromolecules 2, 58–64.
Labib, M., Zamay, A.S., Kolovskaya, O.S., Reshetneva, I.T., Zamay, G.S., Kibbee, R.J., Sattar, S.A., Zamay, T.N., Berezovski, M.V., 2012a. Anal. Chem. 84 (19), 8114–8117.
Labib, M., Zamay, A., Kolovskaya, O.S., Reshetneva, I.T., Zamay, G.S., Kibbee, R., Sattar, S.A., Zamay, T.N., Berezovski, M.,V., 2012b. Anal. Chem. 84, 8966–8969.
Lee, K., Runyon, M., Herrman, T.J., Phillips, R., Hsieh, J., 2015. Food Control 47 (26), 24–276.
Li, L., Wang, Y., Pan, L., Shi, Y., Cheng, W., Shi, Y., Yu, G., 2015. Nano Lett. 15 (2), 1146–1151.
Luo, C., Lei, Y., Yan, L., Yu, T., Li, Q., Zhang, D., Ding, S., Ju, H., 2012. Electroanalysis 24 (5), 1186–1191.
Ma, J., Jiang, y, Jia, F., Yu, Y., Chen, J., Wang, Z., 2014. J. Microbiol. Method 98, 94–98.
Melling, D., Wilsona, S., Jager, E.W.H., A., 2015. RSC Adv. 5 (10), 84153–84163.
Nasef, H., Beni, V., Ozalp, V.C., O'Sullivan, C.K., 2010. Anal. Bioanal. Chem. 396, 2565–2574.
Pattananuwat, P., Tagaya, M., Kobayashi, T., 2015. Sens. Actuators B: Chem. 209, 186–193.
Peng, H., Soeller, C., Vigar, N., Kilmartin, P.A., Cannell, M.B., Bowmaker, G.A., Cooney, R.P., Travas-Sejdic, J., 2005. Biosens. Bioelectron. 20, 1821–1828.
Peng, H., Soeller, C., Vigar, N.A., Caprio, V., Travas-Sejdic, J., 2007. Biosens. Bioelectron. 22, 1867–1883.
Peng, H., Zhang, L.J., Soeller, C., Travas-Sejdic, J., 2009. Biomaterials 30, 2132–2148.
Salam, F., Tothill, I.,E., 2009. Biosens. Bioelectron. 24, 2630–2636.
Street, G.B., Clarke, T.C., Geiss, R.H., Lee, V.Y., Nazzal, A.I., Pfluger, P., Scott, J.C., 1983. J. Phys. 44-C3, 599.
Svennersten, K., Berggren, M., Dahlforsa, A., Jager, E.W.H., 2011. Lab Chip 11 (19), 3287–3293.
Thompson, L.A., Kowalik, J., Josowicz, M., Janata, J., 2003. J. Am. Chem. Soc. 125, 324–325.
Tlili, C., Korri-Youssoufi, H., Ponsonnet, L., Martelet, C., Jaffrezic-Renault, N.J., 2005. Talanta 68, 131–137.
Truong, L.T.N., Chikae, M., Ukita, Y., Takamura, Y., 2011. Talanta 85, 2576–2580.
Wallace, G.G., Teasdale, P.R., Spinks, G.M., Kane-Maguire, L.A.P., 1997. Conductive Electroactive Polymers: Intelligent Polymer Systems, first ed..
Xu, L.B., Chen, W., Mulchandani, A., Yan, Y.S., 2005. Angew. Chem. Int 44, 6009–6012.
Xu, M., Wang, R., Li, Y., 2015. Talanta 148, 200–208.
Zelada-Guillén, G.A., Sebastián-Avila, J.L., Blondeau, P., Riu, J., Xavier, R.F., 2012. Biosens. Bioelectron. 31, 226–232.
Zelada-Guilln, G.A., Riu, J., Duzgun, A., Rius, F.X., 2009. Angew. Chem. 48, 7334–7337.
Zhu, Y., Chandra, P., Song, K.-M., Ban, C., Shim, Y.B., 2012. Biosens. Bioelectron. 36, 29–34.
Zourob, M., Elwary, S., Turner, A., 2008. Principal of Bacterial Detection, Biosensors, Recognition Receptorsand Microsystems. Springer, New York.